Chemistry & Biology
Article

In Vivo and In Vitro *Trans*-Acylation by BryP, the Putative Bryostatin Pathway Acyltransferase Derived from an Uncultured Marine Symbiont

Nicole B. Lopanik,[1,7] Jennifer A. Shields,[2] Tonia J. Buchholz,[1] Christopher M. Rath,[1,3] Joanne Hothersall,[2] Margo G. Haygood,[4] Kristina Håkansson,[3] Christopher M. Thomas,[2] and David H. Sherman[1,3,5,6,*]
[1]Life Sciences Institute, University of Michigan, Ann Arbor, MI 48109, USA
[2]School of Biosciences, University of Birmingham, Edgbaston, Birmingham B15 2TT, UK
[3]Department of Chemistry, University of Michigan, Ann Arbor, MI 48109, USA
[4]Department of Environmental and Biomolecular Systems, Oregon Health and Science University, Beaverton, OR 97006, USA
[5]Department of Medicinal Chemistry, University of Michigan, Ann Arbor, MI 48109, USA
[6]Department of Microbiology & Immunology, University of Michigan, Ann Arbor, MI 48109, USA
[7]Present address: Department of Biology, Georgia State University, Atlanta, GA 30303, USA
*Correspondence: davidhs@umich.edu
DOI 10.1016/j.chembiol.2008.09.013

SUMMARY

The putative modular polyketide synthase (PKS) that prescribes biosynthesis of the bryostatin natural products from the uncultured bacterial symbiont of the marine bryozoan *Bugula neritina* possesses a discrete open reading frame (ORF) (*bryP*) that encodes a protein containing tandem acyltransferase (AT) domains upstream of the PKS ORFs. BryP is hypothesized to catalyze *in trans* acylation of the PKS modules for polyketide chain elongation. To verify conservation of function, *bryP* was introduced into AT-deletion mutant strains of a heterologous host containing a PKS cluster with similar architecture, and polyketide production was partially rescued. Biochemical characterization demonstrated that BryP catalyzes selective malonyl-CoA acylation of native and heterologous acyl carrier proteins and complete PKS modules in vitro. The results support the hypothesis that BryP loads malonyl-CoA onto Bry PKS modules, and provide the first biochemical evidence of the functionality of the *bry* cluster.

INTRODUCTION

Evidence is mounting that many bioactive natural products isolated from marine invertebrates (e.g., sponges, ascidians, bryozoans) are produced by microbial symbionts (reviewed by Konig et al. [2006], Piel [2004], and Salomon et al. [2004]). Particularly compelling evidence indicates that the bryostatins, ecologically relevant bioactive compounds isolated from the temperate marine bryozoan, *Bugula neritina*, are produced by the uncultured microbial symbiont "*Candidatus* Endobugula sertula" that resides in *B. neritina* (Davidson et al., 2001; Lopanik et al., 2004b; Lopanik et al., 2006b). To date, different populations of *B. neritina*-"*Ca.* Endobugula sertula" have yielded 20 different bryostatins (Lopanik et al., 2004a; Pettit, 1996). Each of these molecules bears an identical polyketide core, but is distinguished by its pendant acyl groups at two positions in the bryolactone ring system. The pharmacological activity of bryostatin 1 has been extensively studied; it has been shown to activate protein kinase C (reviewed by Mutter and Wills [2000]) and exhibits anticancer activity, as well as promise against neurodegenerative disorders, including Alzheimer's disease (Etcheberrigaray et al., 2004; Sun and Alkon, 2005). To date, the National Cancer Institute lists 38 completed, ongoing, or planned clinical trials using bryostatin 1 as a single or combination therapeutic, and its importance as a molecular probe to understand specific neurological disorders is also increasing.

Recently, the 77 kb biosynthetic gene cluster (*bry*) that is putatively responsible for assembly and tailoring of the bryostatins was cloned and sequenced from two geographically distinct sibling species of "*Ca.* Endobugula sertula"/*B. neritina* (Figure 1A) (Davidson and Haygood, 1999; Hildebrand et al., 2004; Sudek et al., 2007). The *bry* genes from the deep-water California (CA) sibling species are positioned on at least two loci of the chromosome, while the gene cluster from the shallow-water North Carolina (NC) sibling species appears to reside on a contiguous fragment of DNA. All evidence suggests that *bry* encodes the enzymes necessary for bryostatin biosynthesis, but, as "*Ca.* Endobugula sertula" has been refractory to cultivation efforts, gene disruption and complementation have not been possible. Portions of *bry* have been shown by PCR to be absent in antibiotic-cured *B. neritina* (Davidson et al., 2001; Lopanik et al., 2006a), and colocalization of 16S rRNA of "*Ca.* Endobugula sertula" and a fragment of the PKS genes using in situ hybridizations on *B. neritina* larvae (Davidson et al., 2001) provide evidence for their bacterial origin. Moreover, analysis of PKS fragments amplified from *B. neritina*-derived "*Ca.* Endobugula sertula" metagenome samples revealed that *bry* is the only biosynthetic locus large enough to specify assembly of bryostatin metabolites (Davidson et al., 2001).

Bacterial type I PKSs are large multifunctional enzymes that produce complex polyketide molecules in an assembly line manner (reviewed by Fischbach and Walsh [2006]). The group of enzymatic domains responsible for one chain elongation step is termed a module. Three enzymatic domains comprise a minimal module in PKS biosynthesis: the acyltransferase (AT), the acyl

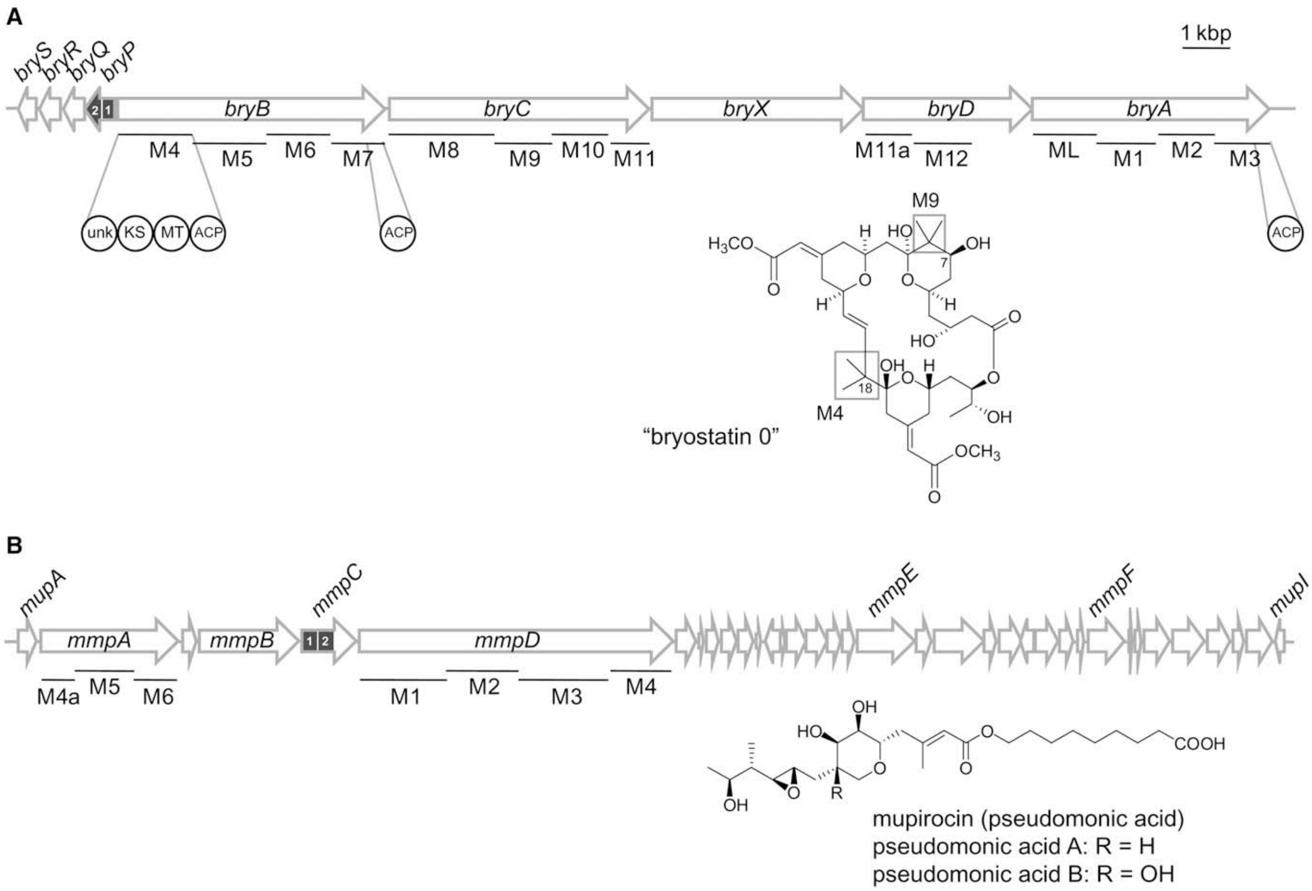

Figure 1. Organization and Orientation of Biosynthetic Gene Clusters and Discrete AT Didomains

(A) Presumed bryostatin gene cluster from shallow-water "*Candidatus* Endobugula sertula"-*B. neritina* populations (Sudek et al., 2007). Enzymatic domains overexpressed in this study are zoomed. Modules putatively responsible for the portions of the bryostatin precursor, "bryostatin 0," are noted.

(B) Mupirocin (PA) gene cluster from *P. fluorescens* NCIMB 10586 (El-Sayed et al., 2003).

Scale bar, 1 kbp for (A) and (B).

carrier protein (ACP), and the ketosynthase (KS). The AT catalyzes covalent linkage of the CoA-activated extender unit onto the ACP, and the KS domain catalyzes condensation of each extender unit, resulting in elongation of the polyketide chain by two carbons. Often, there are additional domains within a module, termed β-keto processing domains, which act to modify the β-carbonyl, the ketoreductase (KR), the dehydratase (DH), and the enoyl reductase. After full extension and reduction of the polyketide chain, it is released in either a cyclized or linear form, typically catalyzed by a thioesterase domain operating at the end of the pathway. Following release from the PKS, the natural product can be further modified by tailoring enzymes, such as oxygenases, methyltransferases (MTs), and glycosyltransferases (reviewed by Rix et al. [2002]).

One significant feature of the putative bryostatin PKS is the absence of AT domains within the polypeptides. Instead, a single ORF (*bryP*) encoding two AT domains is present directly upstream of the PKS genes in the NC-derived gene cluster (Figure 1A) (Sudek et al., 2007). There are several other PKS and hybrid PKS/nonribosomal peptide synthetase (NRPS) clusters that have discrete AT domains (termed "*trans*-AT"), including leinamycin (Cheng et al., 2003), lankacidin (Mochizuki et al., 2003), mupirocin (Figure 1B) (El-Sayed et al., 2003), pederin (Piel, 2002), onnamide (Piel et al., 2004), rhizoxin (Partida-Martinez and Hertweck, 2007), mycosubtilin (Duitman et al., 1999), myxovirescin (Simunovic et al., 2006), virginamycin M (Pulsawat et al., 2007), difficidin (Chen et al., 2006), macrolactin (Chen et al., 2006; Schneider et al., 2007), and bacillaene (Butcher et al., 2007; Moldenhauer et al., 2007). In these AT-less modules, there are well-defined remnants of AT domains that are hypothesized to aid in docking of the *trans*-AT protein, although this has yet to be confirmed experimentally (Nguyen et al., 2008; Tang et al., 2004). The first in vitro experiment demonstrating that a *trans*-AT is able to load malonyl-CoA onto excised ACPs was performed with the discrete AT (LmnG) and ACPs from the leinamycin gene cluster (Cheng et al., 2003). Furthermore, LmnG was shown to load malonyl-CoA onto a tridomain portion of LmnJ (DH-ACP-KR). Subsequent studies have shown that discrete ATs are able to load malonyl-CoA onto cognate discrete and excised ACPs (Calderone et al., 2006, 2007). It is proposed by Nguyen et al. (2008) that discrete AT domains act *in trans*, loading the extender unit onto the ACP of the AT-less module, but this has yet to be demonstrated in vitro with a complete native PKS module.

In addition to *bry*, several other PKS and PKS/NRPS gene clusters encode multiple discrete AT domains. The pederin system from the microbial symbiont of the beetle *Paederus fucipes* has two AT domains on two different ORFs (Piel, 2002), while the bacillaene gene cluster from two *Bacillus* species has three AT domains on three different ORFs (Butcher et al., 2007; Chen et al., 2006; Moldenhauer et al., 2007). The bryostatin gene cluster has two AT domains encoded on a single ORF (BryP), and several other gene clusters also have *trans*-AT didomain ORFs, including the mupirocin gene cluster from *Pseudomonas fluorescens* (*mmpC*) (El-Sayed et al., 2003), the myxovirescin gene cluster from *Myxococcus xanthus* (*taV*) (Simunovic et al., 2006), and the rhizoxin gene cluster from *Burkholderia rhizoxina* (*rhiG*) (Partida-Martinez and Hertweck, 2007). Gene disruption studies of the complete didomain were performed for both *taV* (Simunovic et al., 2006) and *rhiG* (Partida-Martinez and Hertweck, 2007), and, in both cases, secondary metabolite production was completely abolished. Similarly, when the second AT domain of MmpC (AT_2) was deleted from the genome of *P. fluorescens*, no mupirocin was detected in the supernatant of the mutant strain (El-Sayed et al., 2003). Upon complementation with a plasmid bearing *mmpC*, mupirocin production was restored to wild-type levels, demonstrating the necessity of MmpC AT_2 for mupirocin biosynthesis. Although it is clear that the *trans*-AT domains are required for biosynthesis, the purpose of two AT domains on a single ORF remains enigmatic.

In this article, we explore the substrate specificity of BryP in vivo and in vitro. Mono- and didomain constructs of BryP were introduced into *P. fluorescens mmpC* AT_1 and AT_2 deletion mutants, and restoration of mupirocin production for one AT resulted. We investigated the substrate specificity in vitro by assessing the ability of the *bryP*-encoded AT mono- and didomains to transfer malonyl- or methylmalonyl-CoA to a variety of carrier proteins from the bryostatin PKS and other heterologous PKS and NRPS systems. We demonstrate that BryP is able to transfer malonyl-CoA onto the ACP domain of a full native module from the bryostatin PKS. Furthermore, to our knowledge, this work represents the first example of biochemical studies on enzymes from a microbial symbiont-derived natural product biosynthetic pathway.

RESULTS AND DISCUSSION

Sequence and Phylogenetic Analysis of BryP AT_1 and AT_2

The DNA sequences of the shallow-water NC and deep-water CA AT didomain *bryP* are 98.5% identical, and the corresponding amino acid sequences are 96.8% identical (98.4% similar). BryP AT_1 and AT_2 from shallow-water NC populations share only 25.9% identity with each other at the amino acid level, but both domains contain the necessary signature sequences found in functional ATs from fatty acid and polyketide synthases (see Figure S1 available online). Notably, the N-terminal (P/S/T) GQGSQ loop that makes up one side of the active site binding cleft is present in both BryP AT_1 (residues 8–13) and BryP AT_2 (322–327). Additionally, the catalytic dyad (Ser-His) is present in both domains. Considerable investigation during the past few years (Petkovic et al., 2008; Reeves et al., 2001) has enabled prediction of the substrate preference for each AT domain, and an ability to correlate selectivity to key amino acid motifs. Based on multiple sequence alignments, BryP AT_1 shares all characteristics of a malonyl-CoA-specific AT (Figure S1). BLAST analysis revealed that BryP AT_1 is most similar to the PksC AT domain from the bacillaene gene cluster in *Bacillus subtilis* subsp. *subtilis* str. 168 (NP_389591; e value = 8×10^{-77}; 55% identity), and to BaeC from *Bacillus amyloliquefaciens* FZB42 (YP_001421285; e value = 2×10^{-76}; 54% identity). BryP AT_2 is most similar to an AT domain identified in the genome sequence of *Clostridium cellulolyticum* H10 (ZP_01574356.1; e value = 8×10^{-56}; 38% identity), to BaeD, a discrete AT from the bacillaene cluster of *B. amyloliquefaciens* FZB42 (CAG23951.1; e value = 4×10^{-45}; 33% identity [Chen et al., 2006]), and to PedC, a discrete AT encoded in the pederin gene cluster (AAS47559.1; e value = 4×10^{-40}; 34% identity [Piel, 2002]). However, due to lack of a structural model for BryP AT_2 and its closest homologs, the role that specific residues lining the active site pocket play in substrate specificity is more difficult to predict.

Phylogenetic analysis of the amino acid sequences suggests that BryP AT_1 is closely related to AT domains from bacterial FASs (Figure 2). These discrete enzymes utilize malonyl-CoA as a substrate for fatty acid biosynthesis (Hopwood and Sherman, 1990). Other PKS *trans*-AT domains (MmpC AT_2, PedD, RhiG AT_2, LmnG, DifA) form a clade together with BryP AT_1. Interestingly, BryP AT_2 diverges from these FAS-related AT domains, and forms a clade with another group of *trans*-AT domains, including MmpC AT_1 (El-Sayed et al., 2003), RhiG AT_1 (Partida-Martinez and Hertweck, 2007), PedC (Piel, 2002), and BaeD (Chen et al., 2006), which appears to be more closely related to embedded PKS AT domains (Figure 2). While all *trans*-AT PKSs that have been sequenced to date have a discrete AT domain from the former category (e.g., related to FAS AT), only a few have a discrete AT from the latter category (i.e., PKS-embedded AT). Of those with two or three AT domains (e.g., bryostatin [Sudek et al., 2007], mupirocin [El-Sayed et al., 2003], bacillaene [Cheng et al., 2003], myxovirescin A1 [Simunovic et al., 2006], rhizoxin [Partida-Martinez and Hertweck, 2007], and pederin [Piel, 2002]), two AT domains are encompassed on a single ORF for most of these clusters. However, it is unclear why some PKS gene clusters contain more than one *trans*-AT domain. As "*Ca.* Endobugula sertula" remains refractory to laboratory culture, it is not possible to assess function of the two AT domains comprising *bryP* by traditional gene disruption and complementation assays. Instead, a related surrogate system was employed to test functional rescue of AT activity.

Complementation of *P. fluorescens* NCIMB 10586 *mmpC* AT Deletion Mutant by BryP AT_1 and BryP AT_1AT_2

To test the hypothesis that the two *bryP*-encoded AT domains retain and display related functions, we assessed mutant complementation in the mupirocin biosynthetic system from *P. fluorescens* (e.g., production of pseudomonic acid (PA) A [PA-A] [Figure 1B]). Of the two AT domains that comprise MmpC, MmpC AT_2 is most similar to BryP AT_1 phylogenetically (44.4% versus 24.1% to BryP AT_2 amino acid identity), while MmpC AT_1 has a higher similarity to BryP AT_2 (Figure 2; 28.2% versus 23.5% to BryP AT_1 amino acid identity). Bioinformatic analysis has also revealed that MmpC likely contains a third C-terminal domain of unknown function. In-frame deletion of *mmpC*-encoded AT_1 results in the reduction of pseudomonic

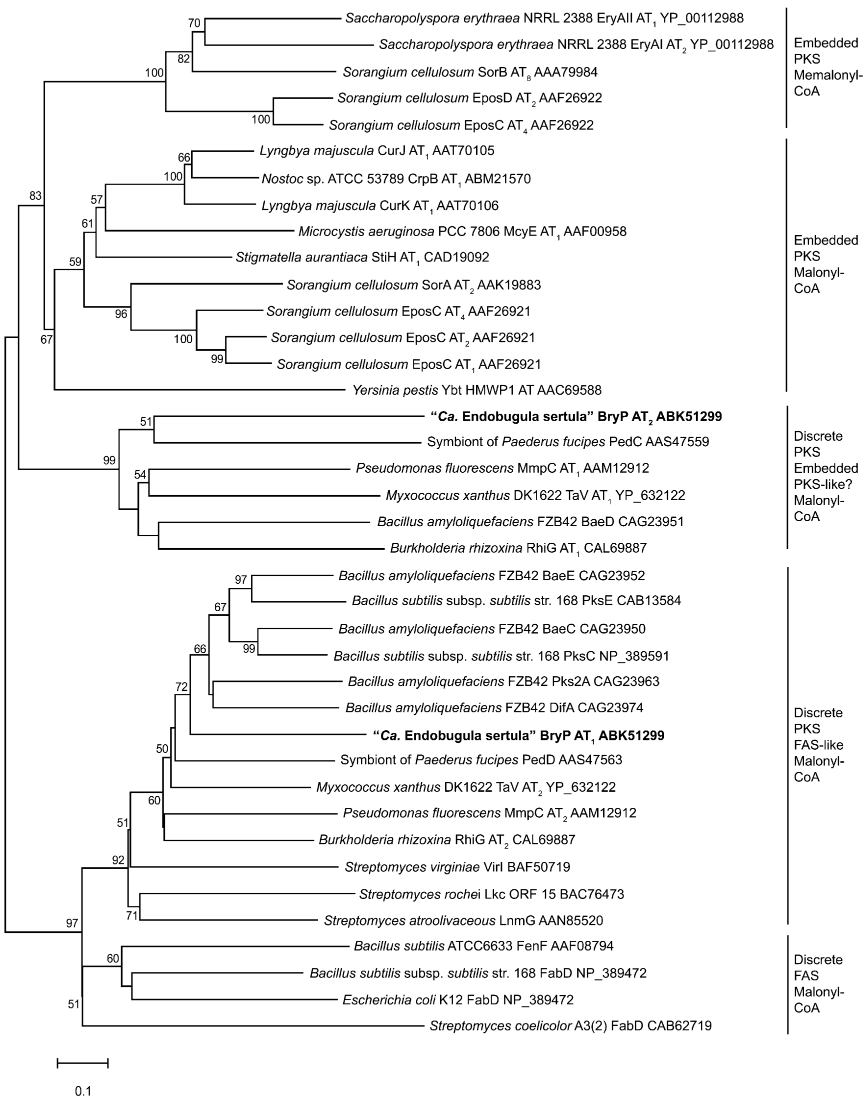

Figure 2. Phylogeny of Discrete PKS ATs in Relation to FAS and Embedded PKS ATs

Minimum evolution tree of amino acid sequences of AT domains from *B. neritina*-"*Ca.* Endobugula sertula" and related PKS and FAS gene clusters. Bootstrap analysis was performed 10,000 times, and nodes with percentages greater than 50% are labeled. Scale bar = 0.1 amino acid substitutions per site. GenBank accession numbers are listed after each sequence, and the sequences utilized in this study are in bold.

acid A (PA-A) to 13.5% of wild-type (WT) *P. fluorescens*, while no PA-A is detected in the *mmpC* AT_2 deletion mutant (Figure 3A). The disk-diffusion bioassays showed that antibiotic activity remaining in the MmpC ΔAT_1 mutant was significant (Figure 3B). Complementation of the Δ*mmpC* AT_1 mutant by BryP AT_1 resulted in restoration of PA-A to approximately 83% of WT levels in the HPLC assays (Figure 3A). Similarly, in the disk-diffusion bioassays, complementation by *bryP* AT_1 restored bioactivity to approximately 70% of WT levels (controls were roughly 30% of WT levels), and the addition of two different concentrations of isopropyl β-D-1-thiogalactopyranoside (IPTG) (0.1 and 0.5 mM) did not affect the bioactivity of the extract (Figure 3B). In contrast, expression of BryP AT_1AT_2 in the ΔMmpC AT_1 mutant resulted in much lower production of PA-A. The addition of IPTG resulted in decreased levels of secondary metabolite production, suggesting that higher levels of BryP AT_1AT_2 can inhibit biosynthesis, possibly due to the formation of a nonfunctional protein-protein complex. However, similar results occurred when plasmid-borne *mmpC* AT_2 was used to complement this mutant (El-Sayed et al., 2003), suggesting that intracellular levels of *trans*-AT may be important during biosynthesis. Interestingly, neither BryP AT_1 nor BryP AT_1AT_2 was able to complement the Δ*mmpC* AT_2 mutant, an in-frame deletion removing only AT_2 (leaving both AT_1 and the third [unknown] domain of MmpC intact). This result was surprising, since BryP AT_1 and MmpC AT_2 cluster together in the FAS-like PKS *trans*-AT group. Since such AT domains clearly can retain the ability to cross-complement (but that this does not correlate with the specific phylotype), it appears that there may be no fundamental difference between the activity of the two AT domains except in the ad hoc way that they may have adapted to their genetic and biochemical context.

In Vitro Substrate Preference of BryP

Sequence analysis of the discrete AT domains suggests that BryP AT_1 should utilize malonyl-CoA as a substrate, as it has several amino acids that are thought to be involved in specificity for this precursor substrate (Met126 and Phe200 *Streptomyces coelicolor* FabD numbering [Keatinge-Clay et al., 2003; Figure S1]). BryP AT_2 also has Phe200 (similar to ATs that mediate malonyl-CoA transfer), but has Leu126 and Ile56 that are typically found in AT domains selective for methylmalonyl-CoA (Keatinge-Clay et al., 2003), suggesting that it may use an alternative substrate. We therefore decided to investigate the substrate specificity of the two AT domains comprising BryP, as well as to determine the ability of the AT domains to transacylate carrier proteins and complete PKS modules. AT-mediated transfer is a two-step reaction (Keatinge-Clay et al., 2003). In the first step, the extender unit substrate (usually either malonyl-CoA or methylmalonyl-CoA) is covalently attached to the active site serine of the AT (termed "loaded") and CoASH is released; in the second step, the extender unit undergoes transesterification from the AT active site serine to the phosphopantetheine prosthetic group of the ACP. In order to investigate the activity of BryP with PKS ACPs and modules, a series of gene constructs were cloned into *Escherichia coli* overexpression vectors, and the purified polypeptides (BryP, as mono- and didomain fusion

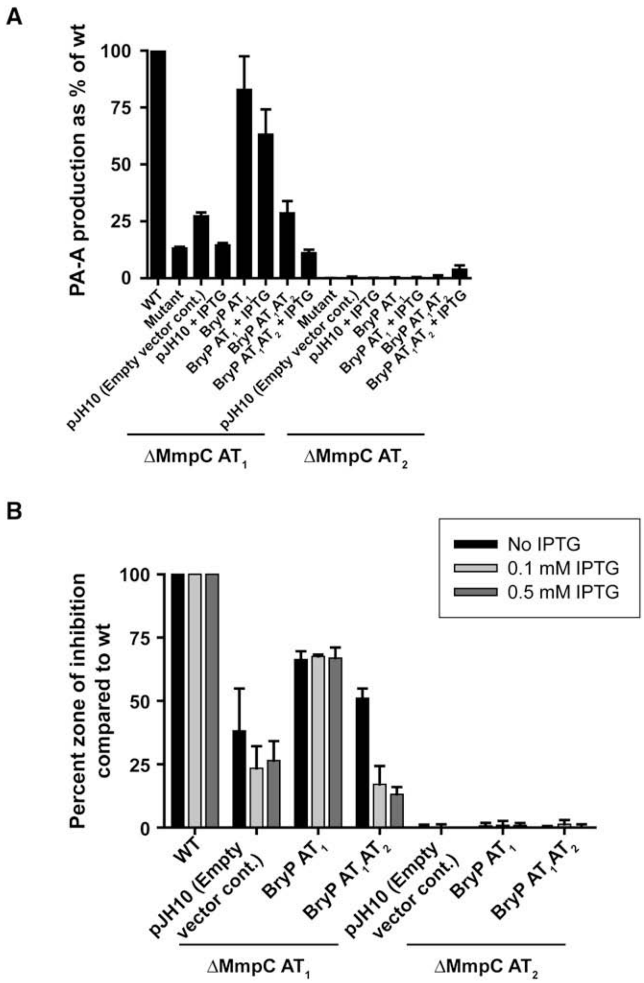

Figure 3. Complementation of *P. fluorescens* MmpC Mutants by BryP AT_1 and BryP AT_1AT_2

(A) HPLC detection of PA-A production. Data are the mean of two experiments where PA-A in supernatants of WT and mutant bacterial cultures were compared, taking WT as 100% and expressing mutant levels relative to this. Error bars indicate differences between duplicate runs. Variations in absolute values between experiments were, on average, about 15%.

(B) Disk diffusion assays of *P. fluorescens* antibiotic activity comparing mutant extracts against *B. subtilis* expressed as a percentage of WT activity, which was taken as 100%, as in (A). Error bars represent standard deviations.

proteins) employed for in vitro assays (see Supplemental Data for details).

The acyl-CoA substrate loading preference of the BryP variants and their ability to transfer the substrates to an ACP from the bryostatin gene cluster (BryB M7 ACP) was assessed. BryP AT_1 was able to transfer [^{14}C]-malonyl-CoA onto *holo* BryB M7 ACP, but not onto the *apo* protein (Figure S2). In addition, no radioactivity was detected from the *holo* BryB M7 ACP that was incubated in the presence of [^{14}C]-malonyl-CoA or [^{14}C]-methylmalonyl-CoA but lacking BryP AT_1, demonstrating that BryB M7 ACP is not able to self-acylate with either substrate. Substrate competition experiments were performed by incubating BryP AT_1 alone or with BryB M7 ACP with a mixture of [^{14}C]-labeled and unlabeled malonyl-CoA and methylmalonyl-CoA. The relative amount of labeling of each protein after SDS-PAGE autoradiography suggests that BryP AT_1 prefers to load and transfer to BryB M7 ACP malonyl-CoA over methylmalonyl-CoA (Figure 4A). The other BryP constructs (BryP AT_1AT_2 and three BryP AT_2 constructs [32, 37, and 47; see Supplemental Data]) were also able to transfer [^{14}C]-malonyl- and [^{14}C]-methylmalonyl-CoA to BryB M7 ACP, although it is evident that more malonyl-CoA is transferred than methylmalonyl-CoA in the same amount of time (20 min) (Figure 4B). In a time course experiment, there was no apparent difference in the amount of labeling of both BryP AT_1 and BryB M7 ACP, suggesting that malonate is not released (e.g., hydrolyzed) from the ACP phosphopantetheine arm after 60 min (data not shown). There was no significant difference in the activity of BryP AT_1 in the range of pH tested (data not shown). In addition, there was no difference detected in the activity of BryP AT_1 at pH 7.4 with and without EDTA and dithioerythritol (DTE). The kinetic parameters of BryP AT_1 transferring varying concentrations of malonyl-CoA to BryB M7 ACP were determined. The K_M was calculated to be 7 μM (±0.6 SE) and k_{cat}/K_M was 0.1 $\mu M^{-1} s^{-1}$ (Figure 4C). Because of the decreased solubility of BryB M7 ACP at high concentrations, kinetic experiments that varied its concentration were not performed. The K_M value of BryP AT_1 with malonyl-CoA as the substrate (7 μM) is a little more than five times lower than the value reported for FenF with MycA ACP_2, but the k_{cat} value is ~24 times less than FenF (Aron et al., 2007). Both the K_M and k_{cat} values are much lower than those calculated for the *S. coelicolor* and *E. coli* FAS MAT and ACP (Szafranska et al., 2002), suggesting that, although BryP AT_1 has a low turnover rate, it has a high affinity for malonyl-CoA.

Fourier transform ion cyclotron mass spectrometry (FT-ICR MS) was employed to qualitatively confirm the types of substrates loaded from a pool of acyl-CoAs and to verify the predicted active-site serine of BryP AT_1. Briefly, BryP AT_1 was incubated with an equimolar mixture of malonyl-, methylmalonyl-, acetyl-, and propionyl-CoA, and analyzed intact by FT-ICR MS. Three peaks were detected in the repeating isotope pattern of the loaded BryP AT_1 (Figure 4D, top panels). For clarity, the mass shift in the +37 charge state is used in the following discussion, although similar shifts in mass were apparent for all charge states observed. Unloaded BryP AT_1 at the expected mass was observed in the sample, as well as BryP AT_1 with a shift in *m/z* of 2.25 or 83.2 Da, likely due to the addition of malonyl-CoA. Additionally, a shift in *m/z* of 2.73 in the +37 charge state was observed, correlating to the addition of 101 Da, and the loading of methylmalonyl-CoA. The control reaction resulted in only unloaded BryP AT_1 (Figure 4D, bottom panels). In a subsequent experiment, BryP AT_1 was subjected to proteolytic digestion prior to FT-ICR MS analysis to ensure that loading occurs on the predicted active site serine residue. A Glu-C-derived peptide, SHKPSYVAGH**S**LGE, was identified by MS/MS in the malonyl- and methylmalonyl-loaded forms. A partial tryptic peptide, TQFTQPALYIINALSFLDKIELESHKPSYVAGH**S**LGEYNALFAAGAFDFLTGLK, was also identified by MS/MS in the malonyl- and methylmalonyl-loaded forms. The predicted active site serine (bold) was determined to be the modified residue in both cases.

LC/MS was used to investigate acyl group transfer from BryP AT_1 to another Bry ACP, BryA M3 ACP (Figure 1A). Both proteins were incubated together in the presence or absence (control) of

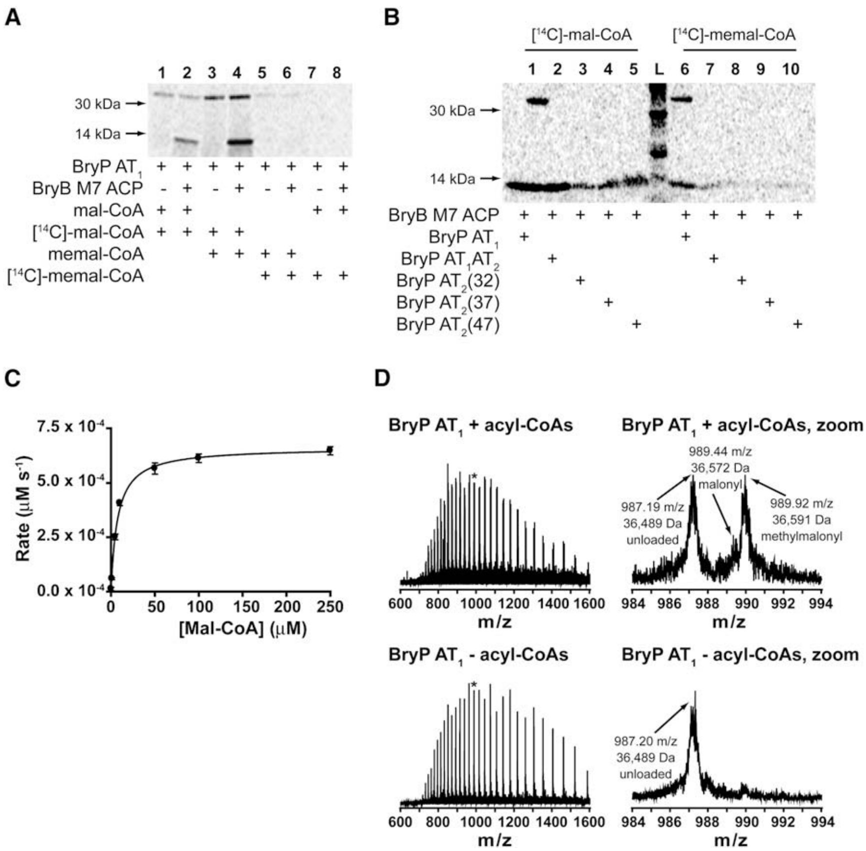

Figure 4. Substrate Preference of BryP Constructs

(A) Autoradiography of SDS-PAGE of BryP AT_1 substrate preference experiment. Lanes 1 and 2, malonyl-CoA/[^{14}C]-malonyl-CoA; lanes 3 and 4, methylmalonyl-CoA/[^{14}C]-malonyl-CoA; lanes 5 and 6, methylmalonyl-CoA/[^{14}C]-methylmalonyl-CoA; and lanes 7 and 8, malonyl-CoA/[^{14}C]-methylmalonyl-CoA. Lanes 1, 3, 5, and 7 contain BryP AT_1 only, and lanes 2, 4, 6, and 8 contain BryP AT_1 and BryB M7 ACP.

(B) Autoradiography of SDS-PAGE of BryP constructs loading onto BryB M7 ACP. Lanes 1 and 6, BryP AT_1 + BryB M7 ACP; lanes 2 and 7, BryP AT_1AT_2 + BryB M7 ACP; lanes 3 and 8, BryP AT_2(32) + BryB M7 ACP; lanes 4 and 7, BryP AT_2(37) + BryB M7 ACP; lanes 5 and 10, BryP AT_2(47) + BryB M7 ACP; and lane L, ladder. Lanes 1–5, [^{14}C]-malonyl-CoA; lanes 6-10, [^{14}C]-methylmalonyl-CoA.

(C) Kinetics of BryP AT_1 loading [^{14}C]-malonyl-CoA onto BryB M7 ACP. Reactions and no-enzyme controls were run in triplicate.

(D) FT-ICR MS analysis (+37 charge state) of full BryP AT_1 incubated with a mixture of acyl-CoAs (top panels) or no substrate (bottom panels). Asterisk indicates peak that is magnified (right panels).

equimolar amounts of acetyl-, malonyl-, methylmalonyl-, and propionyl-CoA. Experiments in the absence of BryP AT_1 showed that the *holo* ACP did not self-load to an appreciable degree (data not shown). In the presence of BryP AT_1 and the acyl-CoAs, BryA M3 ACP peaks increased in mass by 5.1 *m/z* in the +17 charge state, an 86.7 Da mass increase consistent with a preference for malonyl-CoA (Figure 5). An additional peak with a mass shift of 179 Da is observed in the LC-MS data; this is likely α-*N*-6-phosphogluconoylation, a common posttranslational modification observed on fusion proteins with a 6× His affinity tag (Geoghegan et al., 1999). This additional peak exhibits the same mass shift and preference as the *holo* ACP.

Taken together, these data suggest that BryP AT_1 can load both malonyl- and methylmalonyl-CoA (Figure 4), but that malonate is preferentially transferred to the Bry ACPs. The preference for malonyl-CoA over methylmalonyl-CoA has been demonstrated for other *trans*-AT gene clusters. In vitro assays with the myxovirescin gene cluster from *Myxococcus xanthus* DK1622 *trans*-AT didomain (TaV) (Simunovic et al., 2006) have shown that TaV AT_2 (which is a FAS-like *trans*-AT [Figure 2]) prefers malonyl-CoA over methylmalonyl-CoA, acetyl-CoA, and propionyl-CoA (Calderone et al., 2007). In addition, TaV AT_2 was able to acylate both discrete and embedded ACP domains from the gene cluster (Calderone et al., 2007). No in vitro assays were performed on TaV AT_1 (Calderone et al., 2007), which is more similar to BryP AT_2 (Figure 2). The *trans*-AT associated with the bacillaene cluster in *B. subtilis* (PksC) (Butcher et al., 2007), which forms a clade with BryP AT_1 (Figure 2), was also shown to preferentially load malonyl-CoA over acetyl-CoA and methylmalonyl-CoA, and transfer malonyl-CoA onto a cognate, discrete ACP (AcpK) (Calderone et al., 2006).

BryP Exhibits Flexibility for Transferring Malonate onto ACPs

The mono- and didomain constructs of BryP were assayed for their ability to transfer substrates onto an ACP from another PKS (pikromycin PikAIII M5 ACP [Xue et al., 1998]), and a peptidyl carrier protein (PCP) from an aminocoumarin (clorobiocin) biosynthetic gene cluster (Pojer et al., 2002). BryP AT_1 transferred [^{14}C]-malonyl-CoA onto a variety of carrier proteins, including the BryB M7, PikAIII M5 ACPs, as well as the *holo* (but not the *apo*) forms of CloN5 (Figure S2). The BryP didomain (BryP AT_1AT_2) and the didomain single mutants BryP $AT_1{}^{\circ}AT_2$ and BryP $AT_1AT_2{}^{\circ}$ were able to catalyze loading of each of the carrier proteins presented. The double mutant BryP $AT_1{}^{\circ}AT_2{}^{\circ}$, as expected, did not catalyze acyl transfer to any of the carrier proteins. One BryP AT_2 construct (37) was also able to catalyze transfer of malonyl-CoA to each of the carrier proteins (data not shown). The flexibility of BryP in transferring malonate to ACPs from two PKS gene clusters (bryostatin and pikromycin) was similar to that of FenF, a discrete FAS-like AT in the mycosubtilin gene cluster (Duitman et al., 1999). FenF did not exhibit significant preference in vitro for the substrate (malonyl-CoA) ACP compared to the loading (palmitoyl-CoA) ACP in MycA (Aron et al., 2007). Conversely, while BryP was also able to transfer malonate onto a PCP from the clorobiocin biosynthetic gene

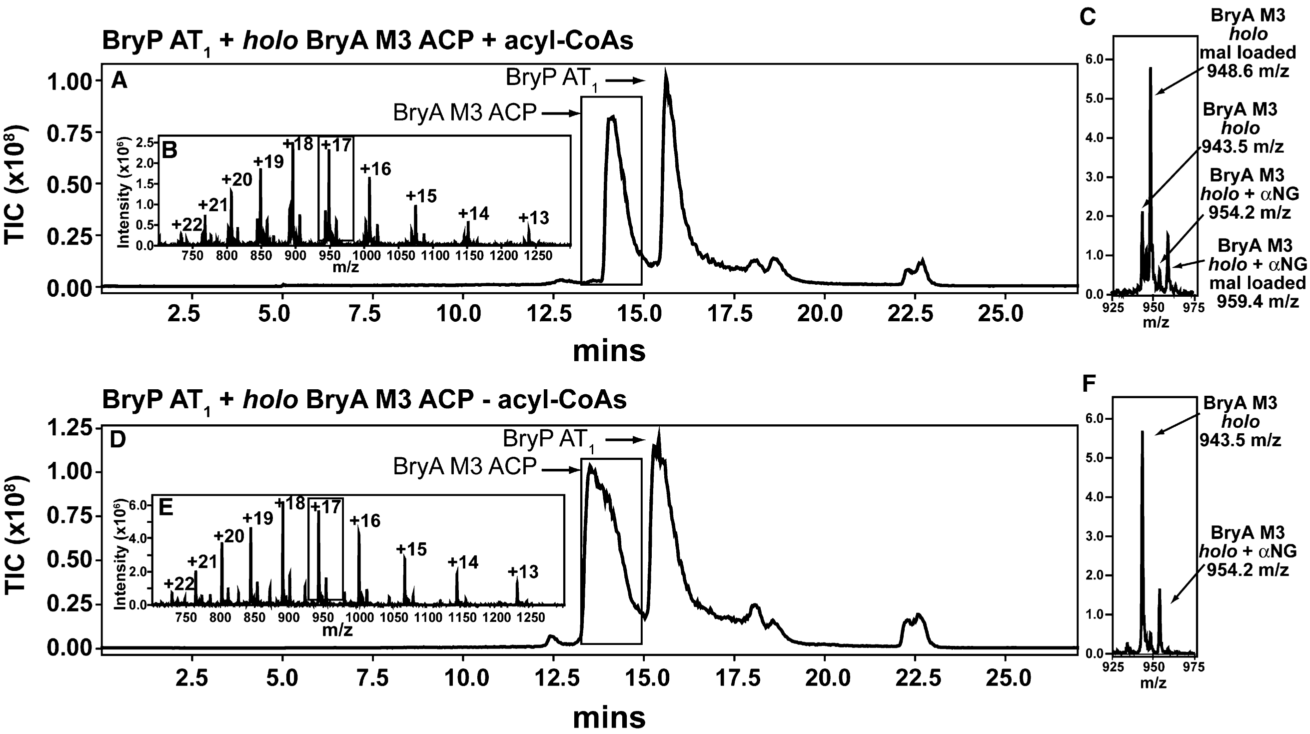

Figure 5. LC/MS Analysis of BryP AT_1 Transfer of acyl-CoAs to *holo* BryA M3 ACP

Reactions with (A–C) and without (D–F) acyl-CoAs are shown.

(A and D) Reversed-phase HPLC TIC chromatogram.

(B and E) Zoom of full spectrum.

(C and F) Zoom on single charge state with assignments. mal, malonyl; αNG, α-N-6-phosphogluconoylation.

(Figure S3), FenF was eight times less efficient loading malonyl-CoA onto one of the PCP domains in MycA (Aron et al., 2007). Moreover, the discrete AT (LnmG) in the leinamycin gene cluster was not able to load malonyl-CoA onto an excised PCP from that PKS/NRPS gene cluster (Cheng et al., 2003), suggesting that either the PCP domain is unable to bind to malonyl-CoA, or that the discrete ATs are unable to recognize or interact with the PCP. As both the hybrid PKS/NRPS leinamycin and mycosubtilin gene clusters contain ACP and PCP domains, it would be advantageous for the discrete ATs to discriminate between the two types of carrier proteins to avoid biosynthetic derailment by acylating the incorrect thiolation domain. However, because the bryostatin gene cluster is only composed of PKS modules, BryP may not have evolved to selectively interact with ACP versus PCP domains.

BryP-Catalyzed Acyl Transfer onto PKS Modules from the Pikromycin, Erythromycin, and Bryostatin Gene Clusters

A previous study demonstrated the ability of the *S. coelicolor* FAS MAT to catalyze transfer of malonyl-CoA onto the ACP of an EryAIII module 6 AT° mutant (Kumar et al., 2003). We decided to extend this type of *trans*-AT substrate delivery analysis using BryP toward a series of PKS modules, including PikAIV M6 (Pik module 6), EryAIII M6, and BryB M4. BryP AT_1 was not able to load malonyl- or methylmalonyl-CoA onto the PikAIV M6 AT° module (Figure 6A), the native substrate of which is methylmalonyl-CoA (Xue et al., 1998). The WT PikAIV M6 was able to self-load and transfer methylmalonyl-CoA, but not malonyl-CoA. Similarly, WT EryAIII M6 was able to self-load methylmalonyl-CoA (its native substrate [Donadio et al., 1991]) (data not shown), but not malonyl-CoA (Figure 6B). In contrast to the PikAIV M6 AT°, BryP AT_1 was able to effectively transfer malonyl-CoA onto EryAIII M6 AT° (Figure 6). Most significantly, BryP AT_1 was able to transfer [^{14}C]-malonyl-CoA onto the *holo* form of the native module BryB M4, but was unable to do so onto the *apo* preparation of BryB M4 (Figure 6B). The BryP AT didomain was able to transfer malonyl-CoA onto both EryAIII M6 AT° and the native module BryB M4 (Figures 7A and 7B). Both single-mutant BryP AT didomain proteins were able to load malonyl-CoA onto these individual modules, although, based on relative signal strengths of the BryP AT_1AT_2 point mutants, it appears that AT_1 is more active than AT_2 (Figure 7B, lanes 4, 5, 11, and 12). The BryP AT double mutant was not able to transfer malonyl-CoA onto the module. Neither BryP AT_1 nor the didomain was able to transfer methylmalonyl-CoA onto either EryAIII M6 AT° or the native BryB M4 module (Figure 7C). Interestingly, BryP AT_2(37) was able to transfer methylmalonyl-CoA onto the EryAIII M6 AT° module, but was unreactive toward BryB M4 (Figure 7C, lane 7). In vivo, these *trans*-ATs are hypothesized to acylate ACP domains that are part of a multidomain module. While the mono- and didomain constructs of BryP were able to transfer malonyl-CoA onto modules BryB M4 and EryAIII M6 AT° (Figures 6B and 7B), BryP AT_1 was unable to transfer

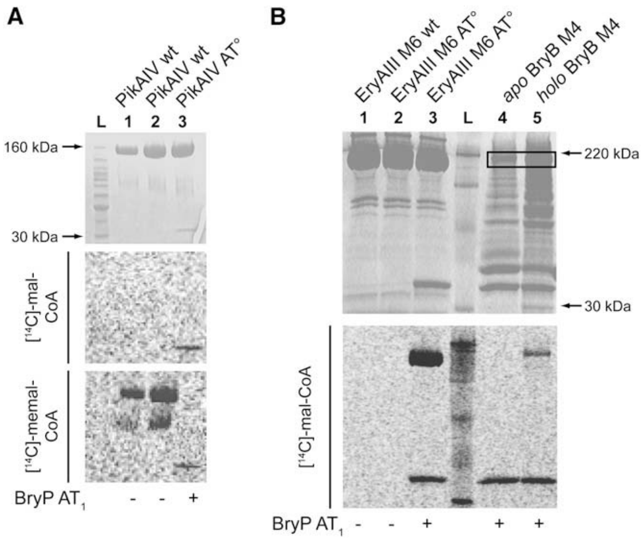

Figure 6. Autoradiography of SDS-PAGE of PKS Module Loading by BryP AT_1

(A) Loading of PikAIV M6 WT and AT°. Lanes 1 and 2, PikAIV M6 WT + BryP AT_1; lane 3, PikAIV M6 AT° + BryP AT_1; and lane L, ladder. Substrate for middle panel is [^{14}C]-malonyl-CoA, and substrate for lower panel is [^{14}C]-methylmalonyl-CoA.

(B) Loading of EryAIII M6 WT and AT°, and BryB M4 with [^{14}C]-malonyl-CoA by BryP AT_1. Lane 1, EryAIII M6 WT + no BryP AT_1; lane 2, EryAIII M6 AT° + no BryP AT_1; lane 3, EryAIII M6 AT° + BryP AT_1; lane L, ladder; lane 4, *apo* BryB M4 + BryP AT_1; and lane 5, BryB M4 + BryP AT_1.

malonyl-CoA onto PikAIV AT° (Figure 6A). These data suggest that there may be some specificity regarding the interaction between the *trans*-AT and the module.

All of the bryostatins characterized to date have two *gem*-dimethyl groups (at C8 and C18; Figure 1). The modules that are putatively responsible for the assembly of those regions contain MT domains (M4 and M9) (Sudek et al., 2007) that could add either one or two methyl groups to the α-carbon. We were motivated to investigate the substrate preference of the two AT domains of BryP, as they could possibly load different substrates (malonyl-CoA or methylmalonyl-CoA) onto the ACPs from these modules that could then be methylated either once or twice by the embedded MT enzymatic domains, resulting in the geminal dimethylated carbon atoms. Two other natural products that have *gem-C*-dimethyl groups are the mixed PKS/NRPS compounds epothilone (Molnar et al., 2000) and yersiniabactin (Gehring et al., 1998), and both have embedded MT domains within the PKS module, which is responsible for the elongation and modification of the corresponding portion of the molecule. The biosynthetic origins for the methyl groups have been investigated, and, interestingly, two different mechanisms have been described. In yersiniabactin biosynthesis, data from in vivo feeding studies (Gehring et al., 1998) and in vitro assays with purified enzymes (Miller et al., 2002) suggest that the polyketide chain is elongated by malonyl-CoA, and both methyl groups originate from *S*-adenosyl-methionine. However, in epothilone biosynthesis, several lines of evidence, including feeding studies (Gerth et al., 2000) and bioinformatic analysis of the AT domain substrate preference (Molnar et al., 2000; Petkovic et al., 2008), support the hypothesis that methylmalonyl-CoA is incorporated into the polyketide chain by the embedded AT, followed by *C*-methylation on the α-carbon. One of the Bry MT-containing modules was targeted (BryB M4) (Sudek et al., 2007) in efforts to determine the likely mode of methylation. When methylmalonyl-CoA was tested as a substrate, the single BryP AT_2 domain was able to label only EryAIII M6 AT°, the natural substrate of which is methylmalonyl-CoA (Donadio et al., 1991). As neither the BryP didomain nor the BryP AT_1°AT_2 mutant was able to acylate EryAIII M6 AT° with methylmalonyl-CoA, having the additional domain (AT_1) may interfere with the ability of AT_2 to load the module with methylmalonyl-CoA. However, since BryP was not able to load methylmalonyl-CoA onto BryB M4, it seems more likely that the MT adds two methyl groups as in yersiniabactin biosynthesis. The dimethylation at the C-8 and C-18 positions on the growing bryostatin chain elongation intermediate is consistent with the general malonyl-CoA selectivity of all known *trans*-AT domains investigated from various Gram-positive, Gram-negative, and microbial symbiont natural product pathways (Nguyen et al., 2008). This is also consistent with the lack of a methylmalonyl-CoA precursor pool in all known γ-proteobacteria that includes the uncultured bacterial symbiont "*Candidatus* Endobugula sertula," which is responsible for the biosynthesis of the bryostatin anticancer natural products.

SIGNIFICANCE

In this study, we demonstrate that BryP exhibits flexibility when loading malonyl- or methylmalonyl-CoA, but prefers to transfer malonate to excised and modular acyl carrier proteins (ACPs). Furthermore, BryP is able to transfer the predicted extender unit, malonyl-CoA, onto a complete native module from the presumed bryostatin biosynthetic gene cluster. Results from this investigation suggest that the geminal dimethyl groups at C-8 and C-18 on the bryolactone ring system are derived from double *C*-methylation of a malonate extender unit during chain elongation. While several large polyketide synthase (PKS) gene clusters from uncultivated symbiotic microbes have been cloned and sequenced (Partida-Martinez and Hertweck, 2007; Piel, 2002; Piel et al., 2004), this is, to our knowledge, the first instance that a large portion of a PKS gene cluster from an uncultivated symbiotic microbe has been overexpressed and demonstrated to function with cognate enzymatic domains. In vivo assays with *Pseudomonas fluorescens* mupirocin ΔAT mutants showed that BryP is only able to complement one of the AT domain mutant strains. A number of questions remain to be explored about how these domains physically interact with PKS modules and full PKS polypeptides and megacomplexes. Finally, this is the first step toward demonstrating unequivocally that the assigned Bry metabolic system produces the bryostatins.

EXPERIMENTAL PROCEDURES

Sequence and Phylogenetic Analysis of the AT Domains

Shallow and deep *bryP* sequences (Sudek et al., 2007) were analyzed by BLAST (Altschul et al., 1990). The amino acid sequences were aligned with the sequences of other *trans*-AT domains as well as integrated AT domains

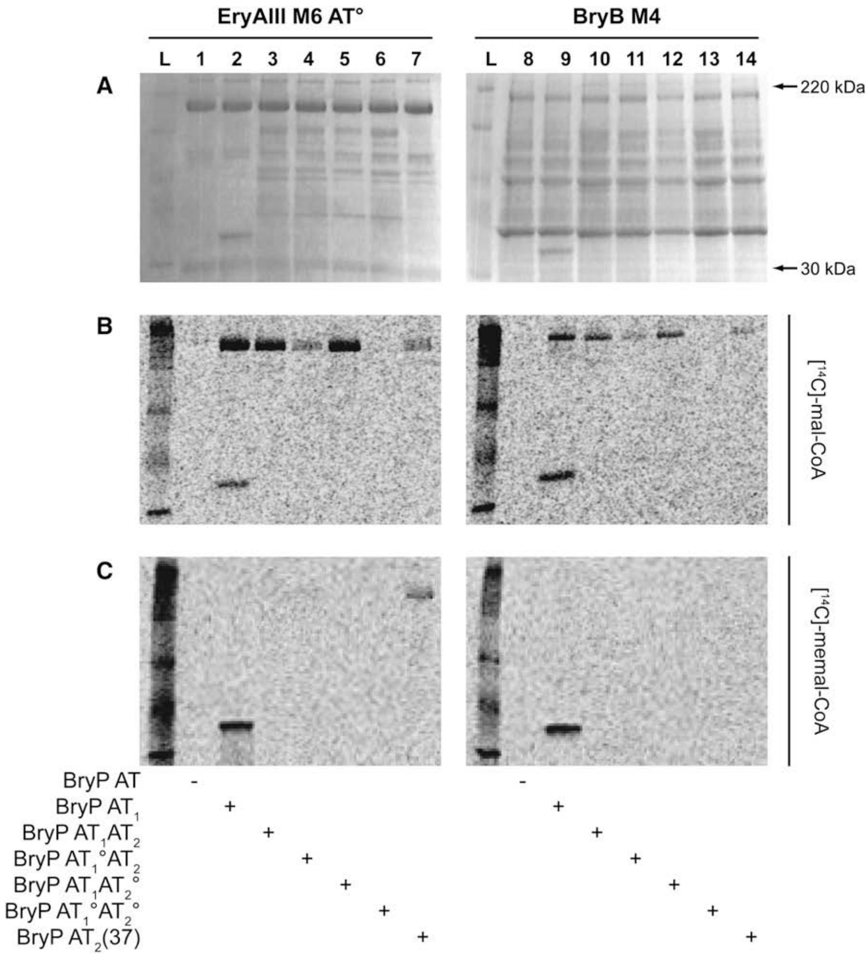

Figure 7. Loading of Substrates onto PKS Modules by BryP

(A–C) (A) Coomassie brilliant blue stained gels, and autoradiography with (B) [^{14}C]-malonyl-CoA and (C) [^{14}C]-methylmalonyl-CoA substrates. Lane L, ladder; lanes 1–7, EryAIII M6 AT°; lanes 8–14, BryB M4. Lanes 1 and 8, no BryP; lanes 2 and 9, BryP AT_1; lanes 3 and 10, BryP AT_1AT_2; lanes 4 and 11, BryP $AT_1°AT_2$; lanes 5 and 12, BryP $AT_1AT_2°$; lanes 6 and 13, BryP $AT_1°AT_2°$, and lanes 7 and 14, BryP AT_2(37).

from PKS gene clusters using ClustalX (Thompson et al., 1997). A minimum evolution phylogenetic tree was generated using *MEGA* version 4 (Tamura et al., 2007). Subjecting the alignment to alternative algorithms (neighbor joining and maximum parsimony) resulted in similar topology.

Generation of *mmpC* AT In-Frame Deletion Mutants in the Mupirocin Producer, *P. fluorescens* NCIMB10856

Construction of an in-frame deletion in MmpC AT_2 has been previously described (El-Sayed et al., 2003). Deletion of MmpC AT_1 was carried out with suicide plasmid pJHAT101 that contains an *mmpC* deletion of 907 bp (23,214–24,120 bp inclusive, database numbering). This creates a frame shift in the remaining MmpC AT_1 sequence such that a 24 codon ORF will deliver ribosomes to the ribosome binding site and ATG start codon at the beginning of the AT_2 domain of *mmpC*. Production of pseudomonic acids by this mutant was verified, suggesting that MmpC AT_2 was still functional.

Construction of *P. fluorescens* expression plasmids.

For *in trans* expression of bryostatin ATs in *P. fluorescens* AT deletion strains, domains were cloned into the IncQ vector pJH10 under the control of the *tac* promoter (El-Sayed et al., 2003). BryP AT_1 was restricted from pNL020 (Table S1) and ligated into pJH10 to give pJS261. The AT didomain (BryP AT_1AT_2) was PCR amplified from a fosmid subclone (MM5_2_BO7) using primers BryP_AT1_F and BryP_AT2_R (Table S2), and cloned into pJH10 to give pJS262. Inserts were verified by sequencing. Complementation plasmids were introduced into the MmpC mutant strains of *P. fluorescens* by conjugation with plasmid-bearing *E. coli* S17-1, as described previously (Hothersall et al., 2007). Positive colonies were screened for metabolite production. Antibiotic disk-diffusion bioassays using *B. subtilis* cultures were used to screen for mupirocin, which is a mixture of PA, dominated by PA-A (90%). Direct quantification of PA-A was performed by HPLC analysis of strain extracts. Both experiments were run in duplicate.

In Vitro Substrate Preference of BryP

Radioactive assays of BryP activity

To determine the ability of BryP to acylate various carrier proteins and PKS modules, each was individually incubated with the BryP proteins and radiolabeled substrate (see cloning and overexpression details in Supplemental Data). In general, the reactions were run in 50 mM HEPES buffer, pH 7.4, 5–10 μM carrier protein or module protein, 1–8 μM BryP protein, and 0.4–0.5 mM substrate. The enzymes were equilibrated at room temperature (RT) for 5 min before the substrate was added. Reactions proceeded for 5–20 min at RT, and were quenched by the addition of 2× SDS-PAGE loading buffer with no reducing agent. The samples were mixed and loaded onto SDS-PAGE gels. After electrophoresis, the gels were stained with either Coomassie blue or SimplyBlue (Invitrogen) stains, and destained. The gels were dried (Bio-Rad), and placed into a phosphoimager cassette (Amersham Biosciences). After 5 days, the phosphoimager screen was scanned, and the images were analyzed.

To determine the substrate preference of BryP AT_1, radiolabeled and unlabeled malonyl- and methylmalonyl-CoA were mixed in separate reactions. [^{14}C]-malonyl- and [^{14}C]-methylmalonyl-CoA (55 mCi/mmol; ARC, Inc.) were mixed with unlabeled malonyl- and methylmalonyl-CoA to result in 0.5 mM total concentration of the substrates. After a 5 min incubation at RT, the amount of labeling on BryP AT_1 (2 μM) and BryB M7 ACP (10 μM) was visualized by SDS-PAGE autoradiography. The BryP AT didomain (BryP AT_1AT_2) and three BryP AT_2 constructs (AT_2[32], AT_2[37], AT_2[47]) were assayed for the ability to transfer [^{14}C]-malonyl-CoA and [^{14}C]-methylmalonyl-CoA (0.5 mM) to BryB M7 ACP (20 μM). As the BryP didomain and BryP AT_2 constructs could not be purified to homogeneity, their concentration could not be determined accurately. A 6 μl aliquot of the eluted protein from the nickel-nitrilotriacetic acid column was used in each reaction; BryP AT_1 was added to a final concentration of 4 μM. The reaction was quenched after 20 min. In a time-course experiment, 7.5 μM of BryB M7 ACP was incubated with 1 μM BryP AT_1 and 0.4 mM [^{14}C]-malonyl-CoA, and the reactions were quenched after 5, 10, 15, 30, and 60 min.

A protein precipitation assay was used to quantify the activity of BryP AT_1 in the presence of BryB M7 ACP. The activity of BryP AT_1 was determined in HEPES buffer (50 mM) with different pH values ranging from 6.0 to 9.2. These assays were conducted by incubating BryP AT_1 (1 nM) with [^{14}C]-malonyl-CoA (0.1 mM) and BryB M7 ACP (50 μM), and measuring the amount of radiolabel bound to BryB M7 ACP after acid precipitation and scintillation counting based on the method previously described (Koppisch and Khosla, 2003). EDTA and DTE (2 mM each) was added to each reaction; one duplicate set of reactions at pH 7.4 was run without EDTA or DTE to determine if they affected BryP AT_1 activity. The reactions and no-enzyme controls (bovine serum albumin [BSA]

10 mg/ml) were run in duplicate. The reaction mixture was equilibrated at RT for 5 min before the enzyme (or BSA) was added, and the reaction proceeded at RT for 5 min. The amount of radiolabel incorporation versus background was compared among the duplicate reactions at the different pHs, and between the pH 7.4 samples run with and without DTE and EDTA.

The reaction kinetics of BryP AT_1 with malonyl-CoA and purified BryB M7 ACP were determined using the TCA precipitation method at pH 7.4. The final concentration of BryP AT_1 was 1 nM, and the final concentration of BryB M7 ACP was 50 μM. The concentration of [^{14}C]-malonyl-CoA varied from 0.2 to 250 μM. The loading reaction proceeded for 5 min on ice, after which the reaction was quenched. The reaction and controls (1 nM BSA) were performed in triplicate. Kinetic parameters were not obtained for varying concentrations of BryB M7 ACP, as this protein would precipitate out of solution at high concentrations.

FT-ICR MS analysis of BryP AT_1

BryP AT_1 (5 μM) was reacted with a pool of 250 μM acetyl-, malonyl-, methylmalonyl-, and propionyl-CoA in 50 mM HEPES (pH 7) buffer and 1 mM TCEP. After incubation for 30 min, samples were acidified with 1% formic acid. Intact protein samples were desalted with Handee Microspin columns (Pierce) packed with 20 μl of 300 Å polymeric C4 resin (Vydac). Samples were loaded onto the columns and washed with 30 column volumes of 0.1% formic acid prior to elution with 10 column volumes of 50% acetonitrile plus 0.1% formic acid. Intact protein samples were analyzed by an FT-ICR MS (APEX-Q with Apollo II ion source and actively shielded 7T magnet; Bruker Daltonics). Data was gathered from *m/z* 250–2000 utilizing direct infusion electrospray ionization in positive ion mode. Electrospray was conducted at 3600 V with 24–60 scans per spectra utilizing 0.5 s external ion accumulation in the hexapole prior to analysis in the FT-ICR using a loop value of 15. All CID MS/MS was performed external to the FT-ICR cell with quadrapole mass selection. In order to confirm that the modification occurred on the active site serine, BryP AT_1 was then subjected to proteolytic digestion after reaction with the acyl CoA pool and FT-ICR MS analysis. Glu-C (Worthington Biochemical) or trypsin (Promega) (1/100 [w/w]) was added to the samples, and digestion proceeded for 4 hr at 37°C. Proteolytic peptides were desalted as above with the exception that C18 resin was utilized. FT-ICR MS analysis was performed as above, except that the loop value was 4 and the ion accumulation time was 1 s.

LC-MS analysis of BryA M3 ACP

BryP AT_1 (2 μM) and BryP AT_1 (20 μM) were reacted with a pool of 250 μM acetyl-, malonyl-, methylmalonyl-, and propionyl-CoA. Reactions were incubated for 45 min in 50 mM HEPES (pH 7) and 1 mM TCEP, and were quenched by diluting 2× in 6 M urea, 100 mM HEPES (pH 6). A 10 μl sample of this mixture was analyzed by LC-MS with a Shimadzu LCMS-2010EV (Columbia, MD) after separation on a PLRP-S 2 × 50 mm, 4000 Å, 8 μm polymeric RP-HPLC column (Varian, Palo Alto, CA) heated to 50°C. Samples were desalted online for 5 min with 95% buffer A (98.9% water, 1% acetonitrile, 0.1% formic acid) and 5% buffer B (1% water, 98.9% acetonitrile, and 0.1% formic acid), followed by gradient elution over 20 min. Profile mode data was gathered from *m/z* 400–2000 utilizing electrospray ionization in positive ion mode.

BryP Transfer to Other ACPs

The ability of BryP AT_1 to acylate a variety of carrier proteins was assayed by in vitro incubation of the proteins with radiolabeled substrates followed by SDS-PAGE autoradiography, as described previously. Purified BryP AT_1 (2 μM) was incubated with both *apo* and *holo* BryB M7 ACP (10 μM), 0.4 mM [^{14}C]-malonyl-CoA, and [^{14}C]-methylmalonyl CoA for 5 min at RT. The ability of the other BryP constructs (BryP AT_1AT_2, BryP AT_2[37], and site mutants BryP $AT_1{}^{\circ}AT_2$, $AT_1AT_2{}^{\circ}$, $AT_1{}^{\circ}AT_2{}^{\circ}$) to load [^{14}C]-malonyl-CoA onto a variety of carrier proteins was assessed in a similar fashion. The carrier proteins used were BryA M3 ACP (*apo* and *holo*), PikAIII M5 ACP, and CloN5 (*apo* and *holo*). Each purified carrier protein preparation (20 μM) was incubated with the BryP protein and [^{14}C]-malonyl-CoA (0.2 mM) for 10 min at RT. The BryP concentrations added were 4 μM BryP AT_1, 0.9 mg/ml BryP didomains, and 0.6 mg/ml of BryP AT_2(37). The reaction proceeded for 10 min at RT.

BryP Loading onto Modules from the Pikromycin, Erythromycin, and Bryostatin Gene Clusters

WT PikAIV M6 and the AT mutant (PikAIV M6 AT°) were incubated with BryP AT_1 and [^{14}C]-malonyl-CoA or [^{14}C]-methylmalonyl-CoA. WT PikAIV was tested at 5 and 10 μM, and PikAIV AT° was tested at 10 μM. BryP AT_1 (2 μM) was added, and after equilibration, either radiolabeled substrate was added (0.4 mM). After 5 min at RT, the reaction was quenched. Next, BryP AT_1 was assayed with malonyl-CoA and EryAIII M6 AT° or BryB M4. BryP AT_1 (4 μM) and [^{14}C]-malonyl-CoA (0.5 mM) were incubated with EryAIII M6 AT° (10 μM) for 10 min at RT. The amylose resin elutions of BryB M4 were used without further purification; the pooled fractions were assayed at a final concentration of 2.2 mg/ml total (*holo* BryB M4) or 1.1 mg/ml (*apo* BryB M4). The other BryP constructs were tested for their ability to load both malonyl- and methylmalonyl-CoA onto the EryAIII M6 AT° and BryB M4 modules. The final concentration of EryAIII M6 AT° was 5 μM, that of BryP AT_1 was 4 μM, and that of substrate was 0.5 mM. The final concentration of the BryB M4 preparation was 3.3 mg/ml, that of the BryP AT didomain preparations was 0.9 mg/ml, and that of BryP AT_2(37) was 0.6 mg/ml. The reactions were quenched after 15 min at RT.

SUPPLEMENTAL DATA

Supplemental Data include Supplemental Experimental Procedures, Supplemental Results, three figures, two tables, and Supplemental References and can be found with this article online at http://www.chembiol.com/cgi/content/full/15/11/1175/DC1/.

ACKNOWLEDGMENTS

We thank Niels Lindquist for providing sampling and laboratory support, and W. Clay Brown and Jim DelProposto at the LSI High Throughput Protein core facility for generating and screening the BryP didomain and AT_2 overexpression constructs, and for supplying the pRARE-CDF coexpression plasmid. We would like to thank Jeff Kittendorf for cloning the EryAIII M6 construct, Brian Beck for cloning the PikAIV M6 WT and mutant constructs, and Sabine Grüschow for cloning the *sfp* coexpression vector, pSG701. Sylvie Garneau-Tsodikova generously provided purified *apo* and *holo* preparations of CloN5. N.B.L was supported by National Institutes of Health (NIH) National Research Service Award fellowship 5F32CA110636. Research support was generously provided by NIH grant R01 GM076477 and the Hans W. Vahlteich Professorship to D.H.S.

Received: August 5, 2008
Revised: September 18, 2008
Accepted: September 24, 2008
Published: November 21, 2008

REFERENCES

Altschul, S.F., Gish, W., Miller, W., Myers, E.W., and Lipman, D.J. (1990). Basic local alignment search tool. J. Mol. Biol. *215*, 403–410.

Aron, Z.D., Fortin, P.D., Calderone, C.T., and Walsh, C.T. (2007). FenF: servicing the mycosubtilin synthetase assembly line in *trans*. ChemBioChem *8*, 613–616.

Butcher, R.A., Schroeder, F.C., Fischbach, M.A., Straightt, P.D., Kolter, R., Walsh, C.T., and Clardy, J. (2007). The identification of bacillaene, the product of the PksX megacomplex in *Bacillus subtilis*. Proc. Natl. Acad. Sci. USA *104*, 1506–1509.

Calderone, C.T., Kowtoniuk, W.E., Kelleher, N.L., Walsh, C.T., and Dorrestein, P.C. (2006). Convergence of isoprene and polyketide biosynthetic machinery: isoprenyl-S-carrier proteins in the *pksX* pathway of *Bacillus subtilis*. Proc. Natl. Acad. Sci. USA *103*, 8977–8982.

Calderone, C.T., Iwig, D.F., Dorrestein, P.C., Kelleher, N.L., and Walsh, C.T. (2007). Incorporation of nonmethyl branches by isoprenoid-like logic: multiple beta-alkylation events in the biosynthesis of myxovirescin A1. Chem. Biol. *14*, 835–846.

Chen, X.H., Vater, J., Piel, J., Franke, P., Scholz, R., Schneider, K., Koumoutsi, A., Hitzeroth, G., Grammel, N., Strittmatter, A.W., et al. (2006). Structural and functional characterization of three polyketide synthase gene clusters in *Bacillus amyloliquefaciens* FZB 42. J. Bacteriol. *188*, 4024–4036.

Cheng, Y.Q., Tang, G.L., and Shen, B. (2003). Type I polyketide synthase requiring a discrete acyltransferase for polyketide biosynthesis. Proc. Natl. Acad. Sci. USA *100*, 3149–3154.

Davidson, S.K., and Haygood, M.G. (1999). Identification of sibling species of the bryozoan *Bugula neritina* that produce different anticancer bryostatins and harbor distinct strains of the bacterial symbiont ''*Candidatus* Endobugula sertula''. Biol. Bull. *196*, 273–280.

Davidson, S.K., Allen, S.W., Lim, G.E., Anderson, C.M., and Haygood, M.G. (2001). Evidence for the biosynthesis of bryostatins by the bacterial symbiont ''*Candidatus* Endobugula sertula'' of the bryozoan *Bugula neritina*. Appl. Environ. Microbiol. *67*, 4531–4537.

Donadio, S., Staver, M.J., McAlpine, J.B., Swanson, S.J., and Katz, L. (1991). Modular organization of genes required for complex polyketide biosynthesis. Science *252*, 675–679.

Duitman, E.H., Hamoen, L.W., Rembold, M., Venema, G., Seitz, H., Saenger, W., Bernhard, F., Reinhardt, R., Schmidt, M., Ullrich, C., et al. (1999). The mycosubtilin synthetase of *Bacillus subtilis* ATCC6633: a multifunctional hybrid between a peptide synthetase, an amino transferase, and a fatty acid synthase. Proc. Natl. Acad. Sci. USA *96*, 13294–13299.

El-Sayed, A.K., Hothersall, J., Cooper, S.M., Stephens, E., Simpson, T.J., and Thomas, C.M. (2003). Characterization of the mupirocin biosynthesis gene cluster from *Pseudomonas fluorescens* NCIMB 10586. Chem. Biol. *10*, 419–430.

Etcheberrigaray, R., Tan, M., Dewachter, I., Kuiperi, C., Van der Auwera, I., Wera, S., Qiao, L.X., Bank, B., Nelson, T.J., Kozikowski, A.P., et al. (2004). Therapeutic effects of PKC activators in Alzheimer's disease transgenic mice. Proc. Natl. Acad. Sci. USA *101*, 11141–11146.

Fischbach, M.A., and Walsh, C.T. (2006). Assembly-line enzymology for polyketide and nonribosomal peptide antibiotics: logic, machinery, and mechanisms. Chem. Rev. *106*, 3468–3496.

Gehring, A.M., DeMoll, E., Fetherston, J.D., Mori, I., Mayhew, G.F., Blattner, F.R., Walsh, C.T., and Perry, R.D. (1998). Iron acquisition in plague: modular logic in enzymatic biogenesis of yersiniabactin by *Yersinia pestis*. Chem. Biol. *5*, 573–586.

Geoghegan, K.F., Dixon, H.B.F., Rosner, P.J., Hoth, L.R., Lanzetti, A.J., Borzilleri, K.A., Marr, E.S., Pezzullo, L.H., Martin, L.B., LeMotte, P.K., et al. (1999). Spontaneous α-*N*-6-phosphogluconoylation of a ''His tag'' in *Escherichia coli*: The cause of extra mass of 258 or 178 Da in fusion proteins. Anal. Biochem. *267*, 169–184.

Gerth, K., Steinmetz, H., Hofle, G., and Reichenbach, H. (2000). Studies on the biosynthesis of epothilones: the biosynthetic origin of the carbon skeleton. J. Antibiot. (Tokyo) *53*, 1373–1377.

Hildebrand, M., Waggoner, L.E., Liu, H.B., Sudek, S., Allen, S., Anderson, C., Sherman, D.H., and Haygood, M. (2004). bryA: an unusual modular polyketide synthase gene from the uncultivated bacterial symbiont of the marine bryozoan *Bugula neritina*. Chem. Biol. *11*, 1543–1552.

Hopwood, D.A., and Sherman, D.H. (1990). Molecular genetics of polyketides and its comparison to fatty acid biosynthesis. Annu. Rev. Genet. *24*, 37–66.

Hothersall, J., Wu, J., Rahman, A.S., Shields, J.A., Haddock, J., Johnson, N., Cooper, S.M., Stephens, E.R., Cox, R.J., Crosby, J., et al. (2007). Mutational analysis reveals that all tailoring region genes are required for production of polyketide antibiotic mupirocin by *Pseudomonas fluorescens*—pseudomonic acid B biosynthesis precedes pseudomonic acid A. J. Biol. Chem. *282*, 15451–15461.

Keatinge-Clay, A.T., Shelat, A.A., Savage, D.F., Tsai, S.C., Miercke, L.J.W., O'Connell, J.D., Khosla, C., and Stroud, R.M. (2003). Catalysis, specificity, and ACP docking site of *Streptomyces coelicolor* malonyl-CoA:ACP transacylase. Structure *11*, 147–154.

Konig, G.M., Kehraus, S., Seibert, S.F., Abdel-Lateff, A., and Muller, D. (2006). Natural products from marine organisms and their associated microbes. ChemBioChem *7*, 229–238.

Koppisch, A.T., and Khosla, C. (2003). Structure-based mutagenesis of the malonyl-CoA:acyl carrier protein transacylase from *Streptomyces coelicolor*. Biochemistry *42*, 11057–11064.

Kumar, P., Koppisch, A.T., Cane, D.E., and Khosla, C. (2003). Enhancing the modularity of the modular polyketide synthases: transacylation in modular polyketide synthases catalyzed by malonyl-CoA:ACP transacylase. J. Am. Chem. Soc. *125*, 14307–14312.

Lopanik, N., Gustafson, K.R., and Lindquist, N. (2004a). Structure of bryostatin 20: a symbiont-produced chemical defense for larvae of the host bryozoan, *Bugula neritina*. J. Nat. Prod. *67*, 1412–1414.

Lopanik, N., Lindquist, N., and Targett, N. (2004b). Potent cytotoxins produced by a microbial symbiont protect host larvae from predation. Oecologia *139*, 131–139.

Lopanik, N.B., Targett, N.M., and Lindquist, N. (2006a). Isolation of two polyketide synthase gene fragments from the uncultured microbial symbiont of the marine bryozoan *Bugula neritina*. Appl. Environ. Microbiol. *72*, 7941–7944.

Lopanik, N.B., Targett, N.M., and Lindquist, N. (2006b). Ontogeny of a symbiont-produced chemical defense in *Bugula neritina* (Bryozoa). Mar. Ecol. Prog. Ser. *327*, 183–191.

Miller, D.A., Luo, L.S., Hillson, N., Keating, T.A., and Walsh, C.T. (2002). Yersiniabactin synthetase: a four-protein assembly line producing the nonribosomal peptide/polyketide hybrid siderophore of *Yersinia pestis*. Chem. Biol. *9*, 333–344.

Mochizuki, S., Hiratsu, K., Suwa, M., Ishii, T., Sugino, F., Yamada, K., and Kinashi, H. (2003). The large linear plasmid pSLA2-L of *Streptomyces rochei* has an unusually condensed gene organization for secondary metabolism. Mol. Microbiol. *48*, 1501–1510.

Moldenhauer, J., Chen, X.H., Borriss, R., and Piel, J. (2007). Biosynthesis of the antibiotic bacillaene, the product of a giant polyketide synthase complex of the *trans*-AT family. Angew. Chem. Int. Ed. Engl. *46*, 8195–8197.

Molnar, I., Schupp, T., Ono, M., Zirkle, R.E., Milnamow, M., Nowak-Thompson, B., Engel, N., Toupet, C., Stratmann, A., Cyr, D.D., et al. (2000). The biosynthetic gene cluster for the microtubule-stabilizing agents epothilones A and B from *Sorangium cellulosum* So ce90. Chem. Biol. *7*, 97–109.

Mutter, R., and Wills, M. (2000). Chemistry and clinical biology of the bryostatins. Bioorg. Med. Chem. *8*, 1841–1860.

Nguyen, T., Ishida, K., Jenke-Kodama, H., Dittmann, E., Gurgui, C., Hochmuth, T., Taudien, S., Platzer, M., Hertweck, C., and Piel, J. (2008). Exploiting the mosaic structure of *trans*-acyltransferase polyketide synthases for natural product discovery and pathway dissection. Nat. Biotechnol. *26*, 225–233.

Partida-Martinez, L.P., and Hertweck, C. (2007). A gene cluster encoding rhizoxin biosynthesis in ''*Burkholderia rhizoxina*'', the bacterial endosymbiont of the fungus *Rhizopus microsporus*. ChemBioChem *8*, 41–45.

Petkovic, H., Sandmann, A., Challis, L.R., Hecht, H.J., Silakowski, B., Low, L., Beeston, N., Kuscer, E., Garcia-Bernardo, J., Leadlay, P.F., et al. (2008). Substrate specificity of the acyl transferase domains of EpoC from the epothilone polyketide synthase. Org. Biomol. Chem. *6*, 500–506.

Pettit, G.R. (1996). Progress in the discovery of biosynthetic anticancer drugs. J. Nat. Prod. *59*, 812–821.

Piel, J. (2002). A polyketide synthase-peptide synthetase gene cluster from an uncultured bacterial symbiont of *Paederus* beetles. Proc. Natl. Acad. Sci. USA *99*, 14002–14007.

Piel, J. (2004). Metabolites from symbiotic bacteria. Nat. Prod. Rep. *21*, 519–538.

Piel, J., Hui, D.Q., Wen, G.P., Butzke, D., Platzer, M., Fusetani, N., and Matsunaga, S. (2004). Antitumor polyketide biosynthesis by an uncultivated bacterial symbiont of the marine sponge *Theonella swinhoei*. Proc. Natl. Acad. Sci. USA *101*, 16222–16227.

Pojer, F., Li, S.M., and Heide, L. (2002). Molecular cloning and sequence analysis of the clorobiocin biosynthetic gene cluster: new insights into the biosynthesis of aminocoumarin antibiotics. Microbiology *148*, 3901–3911.

Pulsawat, N., Kitani, S., and Nihira, T. (2007). Characterization of biosynthetic gene cluster for the production of virginiamycin M, a streptogramin type A antibiotic, in *Streptomyces virginiae*. Gene *393*, 31–42.

Reeves, C.D., Murli, S., Ashley, G.W., Piagentini, M., Hutchinson, C.R., and McDaniel, R. (2001). Alteration of the substrate specificity of a modular polyketide synthase acyltransferase domain through site-specific mutations. Biochemistry *40*, 15464–15470.

Rix, U., Fischer, C., Remsing, L.L., and Rohr, J. (2002). Modification of post-PKS tailoring steps through combinatorial biosynthesis. Nat. Prod. Rep. *19*, 542–580.

Salomon, C.E., Magarvey, N.A., and Sherman, D.H. (2004). Merging the potential of microbial genetics with biological and chemical diversity: an even brighter future for marine natural product drug discovery. Nat. Prod. Rep. *21*, 105–121.

Schneider, K., Chen, X.H., Vater, J., Franke, P., Nicholson, G., Borriss, R., and Sussmuth, R.D. (2007). Macrolactin is the polyketide biosynthesis product of the pks2 cluster of *Bacillus amyloliquefaciens* FZB42. J. Nat. Prod. *70*, 1417–1423.

Simunovic, V., Zapp, J., Rachid, S., Krug, D., Meiser, P., and Muller, R. (2006). Myxovirescin A biosynthesis is directed by hybrid polyketide synthases/nonribosomal peptide synthetase, 3-hydroxy-3-methylglutaryl-CoA synthases, and *trans*-acting acyltransferases. ChemBioChem *7*, 1206–1220.

Sudek, S., Lopanik, N.B., Waggoner, L.E., Hildebrand, M., Anderson, C., Liu, H.B., Patel, A., Sherman, D.H., and Haygood, M.G. (2007). Identification of the putative bryostatin polyketide synthase gene cluster from "*Candidatus* Endobugula sertula", the uncultivated microbial symbiont of the marine bryozoan *Bugula neritina*. J. Nat. Prod. *70*, 67–74.

Sun, M.K., and Alkon, D.L. (2005). Dual effects of bryostatin-1 on spatial memory and depression. Eur. J. Pharmacol. *512*, 43–51.

Szafranska, A.E., Hitchman, T.S., Cox, R.J., Crosby, J., and Simpson, T.J. (2002). Kinetic and mechanistic analysis of the malonyl CoA: ACP transacylase from *Streptomyces coelicolor* indicates a single catalytically competent serine nucleophile at the active site. Biochemistry *41*, 1421–1427.

Tamura, K., Dudley, J., Nei, M., and Kumar, S. (2007). *MEGA4*: molecular evolutionary genetics analysis (MEGA) software version 4.0. Mol. Biol. Evol. *24*, 1596–1599.

Tang, G.L., Cheng, Y.Q., and Shen, B. (2004). Leinamycin biosynthesis revealing unprecedented architectural complexity for a hybrid polyketide synthase and nonribosomal peptide synthetase. Chem. Biol. *11*, 33–45.

Thompson, J.D., Gibson, T.J., Plewniak, F., Jeanmougin, F., and Higgins, D.G. (1997). The ClustalX Windows interface: flexible strategies for multiple sequence alignment aided by quality analysis tools. Nucleic Acids Res. *24*, 4876–4882.

Xue, Y., Zhao, L., Liu, H.-w., and Sherman, D.H. (1998). A gene cluster for macrolide antibiotic biosynthesis in *Streptomyces venezuelae*: architecture of metabolic diversity. Proc. Natl. Acad. Sci. USA *95*, 12111–12116.

